AAS 26-123

NASH EQUILIBRIUM SOLUTIONS OF THE CONSTRAINED PURSUIT - EVASION GAME

Filippo Sangiorgi[*], Filippo Mascellani[†], Michele Maestrini[‡] and Andrea De Vittori[§]

Geostationary satellites are essential to provide space-based services for civilian and military purposes, such as communications, weather forecasting, and remote sensing. The increasing risk of hostile actions aimed at damaging or destroying the spacecraft necessitates the design of effective evasive maneuvers. To ensure mission objectives are not compromised, this problem is commonly modeled as a constrained pursuit–evasion game, a particular instance of Constrained Differential Games. Although such games naturally arise in many applications, general results on the existence and uniqueness of their solutions are still lacking. In this work, optimal solutions are investigated in the form of Nash equilibrium, where one or both spacecraft are confined within a prescribed latitude–longitude slot. Spacecraft dynamics are modeled in latitudinal coordinates, including perturbations from the J_{22} effect, the third body, and the solar radiation pressure. Positional constraints are enforced via recentered logarithmic barrier functions, which add penalties to the players' objectives. The motion dynamics and the barrier functions lead to strong nonlinearities in the problem treated through Model Predictive Static Programming. This approach allows the strategies of both players to be expressed in analytical closed form, yielding a saddle-point solution, and thereby ensuring equilibrium. Given the non-cooperative nature of the problem and the impossibility of explicitly specifying a desired time frame for the end of the game, a receding time horizon technique is adopted. The simulation results validate the effectiveness and robustness of the proposed method under different initial conditions, path constraints, and control efforts.

I. INTRODUCTION

Pursuit–Evasion Game is a powerful mathematical abstraction, derived from differential game theory [1], for modeling the interaction between two competing players with opposing objectives. Over the past few decades, pursuit–evasion games have found numerous applications in classical aerospace problems, such as aerial combat involving constant-speed [2] and variable-speed maneuvering aircraft [3], air-to-air missiles and high-performance aircraft [4], [5], as well as orbital engagement scenarios with low-thrust coplanar satellites [6], [7]. The goal of the pursuer is to reach the instantaneous position of the evader, acting as a kinetic impactor, while the goal of the evader is to escape from the pursuer or, at least, to delay the capture time. The most common approaches for deriving the actions of the players are Dynamic Programming (DP) and Calculus of Variations

[*]MSc Student, Department of Aerospace Science and Technology, Politecnico di Milano, Via Privata Giuseppe La Masa 34, 20156 Milano, Italy.

[†]PhD Student, Department of Aerospace Science and Technology, Politecnico di Milano, Via Privata Giuseppe La Masa 34, 20156 Milano, Italy.

[‡]Assistant Professor, Department of Aerospace Science and Technology, Politecnico di Milano, Via Privata Giuseppe La Masa 34, 20156 Milano, Italy.

[§]Postdoctoral Researcher, School of Aeronautics and Astronautics, Purdue University, 701 W. Stadium Avenue, West Lafayette, IN 47907, USA

(CoV). In the case of nonlinear dynamics and nonlinear objective functions, DP approach leads to the solution of the Hamilton-Jacobi-Isaacs (HJI) partial differential equations [8], [9], whereas CoV reduces to solving a Two-Point Boundary Value Problem (TPBVP) [10]. When the problem is formulated as a Linear–Quadratic Differential Game, both approaches converge to solving an Algebraic Riccati matrix equation, which is typically addressed using the State-Dependent Riccati equation (SDRE) method, whose applicability to satellite chasing problems has been demonstrated in [11], [12]. Compared to the solution of HJI equations and TPBVPs, this approach offers a computationally efficient alternative for deriving optimal feedback control laws [13], and can be further adapted to Model Predictive Static Programming (MPSP) [14], to obtain iterative closed-form solutions in close-proximity orbital regimes [15]. The present study extends the pursuit-evasion game to the geostationary regime, considering geostationary satellites as the players of the game. These satellites are typically subject to operational constraints that confine them to prescribed orbital slots to ensure safe coexistence with other satellites [16]. Identifying optimal evasive maneuvers in constrained scenarios requires a methodology to properly bound the problem. Although necessary and sufficient conditions for the existence of the solution of Constrained Linear Quadratic Differential Games have been derived in [17], [18] and applied to dynamic duopoly and highway driving problems, the strong nonlinearity of spacecraft dynamics and the need to discretize the extended constrained region associated with the orbital slot preclude their direct application to orbital scenarios. Reinforcement learning and AI-based approaches have also been extensively investigated in recent years for pursuit–evasion games [19]; however, their applicability in constrained orbital scenarios is limited by the absence of representative datasets suitable for training such algorithms. In contrast, interior-point methods represent a mature and well-founded class of techniques for constrained nonlinear programming, with recentered logarithmic barrier functions [20] offering an effective alternative for handling problem constraints while addressing the aforementioned limitations. This work proposes a novel methodology for the derivation of iterative closed-form solutions to constrained pursuit–evasion games in orbital regimes by extending the framework introduced in [15] through the incorporation of path constraints via recentered logarithmic barrier functions. A general formulation of the problem is reported in Section II. Section III provides an overview of the essential tools underlying the numerical model developed in this study. Section IV presents the analytical steps required to derive the players' strategies. Section V describes the main features of the adopted algorithm, and Section VI presents the numerical results obtained using the proposed methodology.

II. PROBLEM FORMULATION

The Constrained Pursuit-Evasion Game is modeled as a Linear Quadratic Differential Game where the objective functions of the players are given by a quadratic combination of the output of the game $\mathbf{Y} \in \mathbb{R}^3$ and of the state $\mathbf{X}_j \in \mathbb{R}^6$ and control variables $\mathbf{U}_j \in \mathbb{R}^3$ of spacecraft j. Nash equilibrium solutions are obtained by formulating the problem as a Zero-Sum Game where each player seeks to optimize its own payoff while simultaneously hindering the opponent [21]. The optimization problem is solved over a finite predicted horizon according to the receding time horizon technique, with the time dependence explicitly indicated by the subscript $(\cdot)$. Path constraints are incorporated inside the objective functions in the form of penalty terms $\mathbf{W}_j \in \mathbb{R}^6$, driving the players away from the boundaries of the admissible set while incentivizing actions that induce constraint violation by the opponent. The enforcement of constraints on spacecraft j is achieved through adjoint variables $\boldsymbol{\mu}_j \in \mathbb{R}^6$, with components set to zero whenever the corresponding constraints are inactive. The expressions of the objective functions are reported as follows, where, by convention, the pursuer

spacecraft is denoted with player 1, while the evader spacecraft is denoted with player 2:

$$\min_{\mathbf{U}_{1,(k)}\in\mathbb{U}_1} J_1 = \frac{1}{2}\mathbf{Y}_{(N)}^T\mathbf{Q}_1\mathbf{Y}_{(N)} + \frac{1}{2}\sum_{k=0}^{N-1}\mathbf{U}_{1,(k)}^T\mathbf{R}_{1,(k)}\mathbf{U}_{1,(k)} - \frac{1}{2}\sum_{k=0}^{N-1}\mathbf{U}_{2,(k)}^T\mathbf{R}_{2,(k)}\mathbf{U}_{2,(k)} + \dots + \sum_{k=0}^{N-1}\boldsymbol{\mu}_{1,(k+1)}^T\mathbf{W}_{1,(k+1)} - \sum_{k=0}^{N-1}\boldsymbol{\mu}_{2,(k+1)}^T\mathbf{W}_{2,(k+1)} \tag{1}$$

$$\max_{\mathbf{U}_{2,(k)}\in\mathbb{U}_2} J_2 = \frac{1}{2}\mathbf{Y}_{(N)}^T\mathbf{Q}_2\mathbf{Y}_{(N)} + \frac{1}{2}\sum_{k=0}^{N-1}\mathbf{U}_{1,(k)}^T\mathbf{R}_{1,(k)}\mathbf{U}_{1,(k)} - \frac{1}{2}\sum_{k=0}^{N-1}\mathbf{U}_{2,(k)}^T\mathbf{R}_{2,(k)}\mathbf{U}_{2,(k)} + \dots + \sum_{k=0}^{N-1}\boldsymbol{\mu}_{1,(k+1)}^T\mathbf{W}_{1,(k+1)} - \sum_{k=0}^{N-1}\boldsymbol{\mu}_{2,(k+1)}^T\mathbf{W}_{2,(k+1)} \tag{2}$$

$$\text{s.t.} \qquad \dot{\mathbf{X}}_j = \mathbf{f}_j(t,\ \mathbf{X}_j,\ \mathbf{U}_j) \qquad \text{for } j = 1, 2$$

where $\mathbf{Q}_1,\ \mathbf{Q}_2 \in \mathbb{R}^{3\times3}$ are the weight matrix associated with the output of the game, $\mathbf{R}_{1,(0)}, \mathbf{R}_{2,(0)} \in \mathbb{R}^{3\times3}$ are those associated with the control effort and $\mathbf{f}_j$ is the dynamics of spacecraft j.

III. PRELIMINARIES

This section provides the fundamental blocks necessary for the derivation of the players' strategies. Specifically, it introduces the equations of motion governing geostationary satellites, the predictive correction on the output of the game, the principles of the receding time horizon technique, and the analytical formulation of logarithmic barrier functions.

Spacecraft Dynamics

The dynamics of the spacecraft is expressed in the Earth Center Earth-Fixed (ECEF) reference frame defined as in Fig. 1a. The state vector $\mathbf{X} = [\ r,\ \lambda,\ \phi,\ \dot{r},\ \dot{\lambda},\ \dot{\phi}\ ]^T$ is written in spherical coordinates, where r is the range, λ is the longitude, defined as the angle between the satellite projection on the equator and the $\hat{\mathbf{I}}$ axis, positive towards East, and ϕ is the latitude, positive towards the Northern Hemisphere. The orbital slot Fig. 1b, is defined as parallelepiped centered in $[\ r_n,\ \lambda_n,\ \phi_n\ ]^T$, whose dimensions depend on the mission constraints of the satellite.

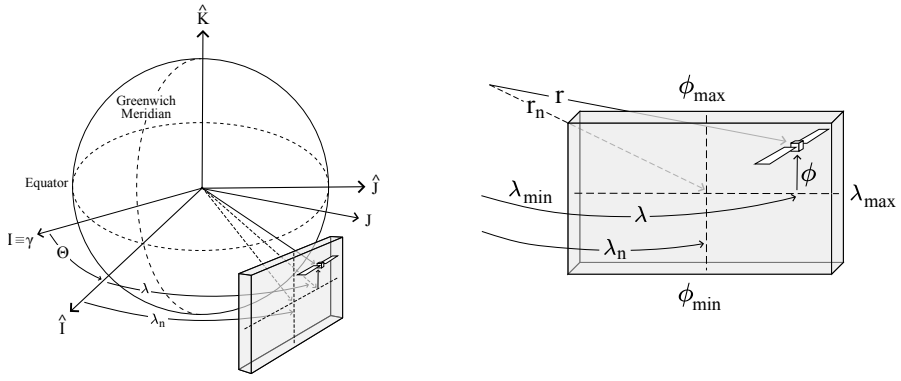

(a) ECEF reference frame.

(b) range-longitude-latitude orbital slot

Figure 1: ECEF reference frame for a geostationary satellite within a prescribed orbital slot.

The equation of motions [22] are reported in Eq. (3), where μ_E is the Earth's gravitational parameter, ω_E is the Earth's rotational speed, $a^p_{\hat{r}}\ a^p_{\hat{\lambda}}\ a^p_{\hat{\phi}}$ are the components of the perturbing accelerations due to the J_{22} effect, third-body perturbation, and solar radiation pressure, and $U_{\hat{r}}\ U_{\hat{\lambda}}\ U_{\hat{\phi}}$ are the components of the control vector:

$$\begin{cases} \ddot{r} = -\dfrac{\mu_E}{r^2} \ + \ r\dot{\phi}^2 \ + \ r(\dot{\lambda}+\omega_E)^2\cos\phi^2 \ + \ a^p_{\hat{r}}(r,\lambda,\phi) \ + \ U_{\hat{r}}(t) \\ \ddot{\lambda} = 2\dot{\phi}(\dot{\lambda}+\omega_E)\tan\phi \ - \ 2\dfrac{\dot{r}}{r}(\dot{\lambda}+\omega_E) \ + \ \dfrac{1}{r\cos\phi}\ a^p_{\hat{\lambda}}(r,\lambda,\phi) \ + \ \dfrac{1}{r\cos\phi}\ U_{\hat{\lambda}}(t) \\ \ddot{\phi} = -2\dfrac{\dot{r}}{r}\dot{\phi} \ - \ (\dot{\lambda}+\omega_E)^2\sin\phi\cos\phi \ + \ \dfrac{1}{r}\ a^p_{\hat{\phi}}(r,\lambda,\phi) \ + \ \dfrac{1}{r}\ U_{\hat{\phi}}(t) \end{cases} \tag{3}$$

Predictive Correction of Game Output in a Satellite Pursuit-Evasion Scenario

This subsection describes the predictive correction methodology [15] as a two-sided pursuit-evasion game. The aim is to iteratively adjust their control inputs so that the relative distance between the pursuer and the evader follows a desired behaviour. Spacecraft dynamics are propagated over time, and small variations in the controls are linearly related to variations in the game output through first-order Taylor expansions, allowing a systematic computation of how changes in the control inputs affect the final distance between the satellites. Section IV provides further details on the predictive correction approach. The dynamics of spacecraft j are discretized in time using the Forward Euler method:

$$\mathbf{X}_{j,(k+1)} = \mathbf{F}_{j,(k)}(\ \mathbf{X}_{j,(k)},\ \mathbf{U}_{j,(k)}\ ) \tag{4}$$

$$= \mathbf{X}_{j,(k)} + \Delta t\ \mathbf{f}_j(\ k\Delta t,\ \mathbf{X}_{j,(k)},\ \mathbf{U}_{j,(k)}\ ) \tag{5}$$

for $k = 0, \ldots, N-1$. The output of the game $\mathbf{Y} \in \mathbb{R}^3$, at the time step (k) is expressed as the vector distance between the position of two satellites, where s/c$_1$ identifies the pursuer and s/c$_2$ the evader:

$$\mathbf{Y}_{(k)} = \mathbf{g}_{(k)}(\ \mathbf{X}_{1,(k)},\ \mathbf{X}_{2,(k)}\ ) \tag{6}$$

$$= \begin{bmatrix}\ \mathbf{I}_{3\times3} & \mathbf{0}_{3\times3}\ \end{bmatrix}\ (\ \mathbf{X}_{1,(k)} - \mathbf{X}_{2,(k)}\ ) \tag{7}$$

for $k = 0, \ldots, N$.

An equilibrium solution is imposed through a correction in the controls $d\mathbf{u}_{j,(k)}$, which determines a variation in the states $d\mathbf{x}_{j,(k)}$ and in the output of the game $d\mathbf{y}_{(k)}$. The corrected values of the game variables are denoted with uppercase letters. The variables of the game computed before the application of the control correction are denoted with lowercase letters.

$$\mathbf{U}_{j,(k)} = \mathbf{u}_{j,(k)} + d\mathbf{u}_{j,(k)} \qquad \mathbf{X}_{j,(k)} = \mathbf{x}_{j,(k)} + d\mathbf{x}_{j,(k)} \qquad \mathbf{Y}_{(k)} = \mathbf{y}_{(k)} + d\mathbf{y}_{(k)}$$

A first-order Taylor expansion of the state at time step $(k+1)$, is performed:

$$\mathbf{X}_{j,(k+1)} = \mathbf{F}_{j,(k)}(\ \mathbf{x}_{j,(k)} + d\mathbf{x}_{j,(k)},\ \mathbf{u}_{j,(k)} + d\mathbf{u}_{j,(k)}\ ) \tag{8}$$

$$\simeq \mathbf{F}_{j,(k)}(\mathbf{x}_{j,(k)},\ \mathbf{u}_{j,(k)}) + \left[\frac{\partial \mathbf{F}_{j,(k)}}{\partial \mathbf{X}_{j,(k)}}\right] d\mathbf{x}_{j,(k)} + \left[\frac{\partial \mathbf{F}_{j,(k)}}{\partial \mathbf{U}_{j,(k)}}\right] d\mathbf{u}_{j,(k)} \tag{9}$$

$$\simeq \mathbf{x}_{j,(k+1)} + \left[\frac{\partial \mathbf{F}_{j,(k)}}{\partial \mathbf{X}_{j,(k)}}\right] d\mathbf{x}_{j,(k)} + \left[\frac{\partial \mathbf{F}_{j,(k)}}{\partial \mathbf{U}_{j,(k)}}\right] d\mathbf{u}_{j,(k)} \tag{10}$$

and therefore the variation of the state of the spacecraft j at the time step $(k+1)$, is straightforward:

$$d\mathbf{x}_{j,(k+1)} = \left[\frac{\partial \mathbf{F}_{j,(k)}}{\partial \mathbf{X}_{j,(k)}}\right] d\mathbf{x}_{j,(k)} + \left[\frac{\partial \mathbf{F}_{j,(k)}}{\partial \mathbf{U}_{j,(k)}}\right] d\mathbf{u}_{j,(k)} \tag{11}$$

Similarly, a first-order Taylor expansion of the output of the game at the time step (k) is computed:

$$\begin{aligned}
\mathbf{Y}_{(k)} &= \mathbf{g}_{(k)}(\ \mathbf{x}_{1,(k)} + d\mathbf{x}_{1,(k)},\ \mathbf{x}_{2,(k)} + d\mathbf{x}_{2,(k)}\ ) && (12)\\
&\simeq \mathbf{g}_{(k)}(\mathbf{x}_{1,(k)},\ \mathbf{x}_{2,(k)}) + \left[\frac{\partial \mathbf{Y}_{(k)}}{\partial \mathbf{X}_{1,(k)}}\right] d\mathbf{x}_{1,(k)} + \left[\frac{\partial \mathbf{Y}_{(k)}}{\partial \mathbf{X}_{2,(k)}}\right] d\mathbf{x}_{2,(k)} && (13)\\
&\simeq \mathbf{y}_{(k)} + \left[\frac{\partial \mathbf{Y}_{(k)}}{\partial \mathbf{X}_{1,(k)}}\right] d\mathbf{x}_{1,(k)} + \left[\frac{\partial \mathbf{Y}_{(k)}}{\partial \mathbf{X}_{2,(k)}}\right] d\mathbf{x}_{2,(k)} && (14)
\end{aligned}$$

Consequently, the variation of the game output at the time step $k = N$ is expressed as follows:

$$d\mathbf{y}_{(N)} = \left[\frac{\partial \mathbf{Y}_{(N)}}{\partial \mathbf{X}_{1,(N)}}\right] d\mathbf{x}_{1,(N)} + \left[\frac{\partial \mathbf{Y}_{(N)}}{\partial \mathbf{X}_{2,(N)}}\right] d\mathbf{x}_{2,(N)} \tag{15}$$

By iteratively substituting the variation of the state of spacecraft $j = 1, 2$ Eq. (11) inside Eq. (15) the predictive correction on the output of the game is obtained:

$$\begin{aligned}
d\mathbf{y}_{(N)} = &\left[\frac{\partial \mathbf{Y}_{(N)}}{\partial \mathbf{X}_{1,(N)}}\right]\left[\frac{\partial \mathbf{F}_{1,(N-1)}}{\partial \mathbf{X}_{1,(N-1)}}\right] \cdot \ \dots \ \cdot \left[\frac{\partial \mathbf{F}_{1,(0)}}{\partial \mathbf{X}_{1,(0)}}\right] d\mathbf{x}_{1,(0)} \ + \dots \\
&+ \left[\frac{\partial \mathbf{Y}_{(N)}}{\partial \mathbf{X}_{2,(N)}}\right]\left[\frac{\partial \mathbf{F}_{2,(N-1)}}{\partial \mathbf{X}_{2,(N-1)}}\right] \cdot \ \dots \ \cdot \left[\frac{\partial \mathbf{F}_{2,(0)}}{\partial \mathbf{X}_{2,(0)}}\right] d\mathbf{x}_{2,(0)} \ + \dots \\
&+ \sum_{k=0}^{N-1} \left(\ \mathbf{B}_{(k)}\ d\mathbf{u}_{1,(k)} \ + \ \mathbf{C}_{(k)}\ d\mathbf{u}_{2,(k)}\ \right)
\end{aligned} \tag{16}$$

where:

$$\begin{aligned}
\mathbf{B}_{(k)} &= \left[\frac{\partial \mathbf{Y}_{(N)}}{\partial \mathbf{X}_{1,(N)}}\right]\left[\frac{\partial \mathbf{F}_{1,(N-1)}}{\partial \mathbf{X}_{1,(N-1)}}\right] \cdot \ \dots \ \cdot \left[\frac{\partial \mathbf{F}_{1,(k+1)}}{\partial \mathbf{X}_{1,(k+1)}}\right]\left[\frac{\partial \mathbf{F}_{1,(k)}}{\partial \mathbf{U}_{1,(k)}}\right] \\
\mathbf{C}_{(k)} &= \left[\frac{\partial \mathbf{Y}_{(N)}}{\partial \mathbf{X}_{2,(N)}}\right]\left[\frac{\partial \mathbf{F}_{2,(N-1)}}{\partial \mathbf{X}_{2,(N-1)}}\right] \cdot \ \dots \ \cdot \left[\frac{\partial \mathbf{F}_{2,(k+1)}}{\partial \mathbf{X}_{2,(k+1)}}\right]\left[\frac{\partial \mathbf{F}_{2,(k)}}{\partial \mathbf{U}_{2,(k)}}\right]
\end{aligned}$$

for $k = 0, ..., N-2$.

Assuming that the initial states are observed with zero errors, their variation is set to zero: $d\mathbf{x}_{1,(0)} = d\mathbf{x}_{2,(0)} = \mathbf{0}$; therefore Eq. (16) is rewritten as follows:

$$d\mathbf{y}_{(N)} = \sum_{k=0}^{N-1} (\ \mathbf{B}_{(k)}\ d\mathbf{u}_{1,(k)} \ + \ \mathbf{C}_{(k)}\ d\mathbf{u}_{2,(k)}) \tag{17}$$

Receding Time Horizon technique

The receding time-horizon technique allows to transform an infinite horizon optimization problem into a finite one [23]. Two temporal domains are introduced in Fig. 2: the first, represented as a segment, corresponds to the predictive horizon with a fixed duration T and a certain discretization Δt; the second, represented as a half-line, corresponds to the time of the game, spanning from t_0 to t_f. When the distance between the two satellites falls below the capture threshold, the game terminates and t_f is set to the capture time. In the case where the evader spacecraft successfully avoids capture, the game continues until a subsequent capture event takes place. If the evolution of the game does not lead to a capture, the two players may establish an equilibrium that allows the

game to potentially last indefinitely.

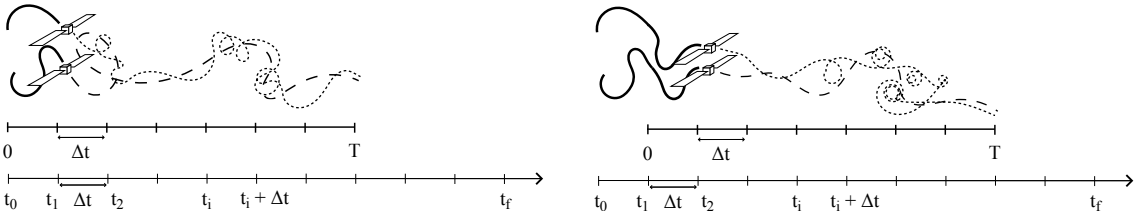

(a) prediction of the evolution of system at $t = t_0$.

(b) prediction of the evolution of system at $t = t_1$.

Figure 2: Mechanics of the Receding Time-Horizon. ⟝ predictive horizon; ⟶ time of the game; —— executed trajectories; ····· s/c 1 predicted trajectory; − − s/c 2 predicted trajectory.

Within the predictive horizon, the states of the players are propagated for $k = 0, \ldots, N$ but only the control corrections corresponding to the time step $k = 0$ are applied, while those associated with subsequent time steps are set to zero:

$$d\mathbf{u}_{1,(k)} = \mathbf{0} \qquad d\mathbf{u}_{2,(k)} = \mathbf{0} \tag{18}$$

for $k = 1, \ldots, N-1$.

As a consequence, the variation in the output of the game Eq. (17) can be expressed as a function of only the control corrections at the first time step of the predictive horizon:

$$d\mathbf{y}_{(N)} = \mathbf{B}_{(0)}\, d\mathbf{u}_{1,(0)} \;+\; \mathbf{C}_{(0)}\, d\mathbf{u}_{2,(0)} \tag{19}$$

This assumption represents the central core of the MPSP framework because it allows to transform a dynamic game into a static one, preserving the differential nature of the game.

Logarithmic Barrier Functions

A Logarithmic Barrier Function [20], $\boldsymbol{\mathcal{L}}(\mathbf{X}) \in \mathbb{R}^6$ is used to confine a generic state $\mathbf{X}$ between a minimum and a maximum value $\mathbf{X}_{\text{min}} \leq \mathbf{X} \leq \mathbf{X}_{\text{max}}$, as follows:

$$\mathcal{L}(X_i)_i = -\ln\left(X_{i,\text{max}} - X_i\right) - \ln\left(X_i - X_{i,\text{min}}\right) \tag{20}$$

for the vector component $i = 1, \ldots, 6$.

In a one-dimensional representation this function is convex, tends to infinity as the constrained variable approaches the limit values, and reaches its minimum in the center of the constraint interval Fig. 3a. $\boldsymbol{\mathcal{L}}(\mathbf{X})$ is then recentred through the gradient as follows:

$$\mathbf{H}(\mathbf{X}, \mathbf{X}_0) = \boldsymbol{\mathcal{L}}(\mathbf{X}) - \boldsymbol{\mathcal{L}}(\mathbf{X}_0) - \nabla\boldsymbol{\mathcal{L}}(\mathbf{X}_0)^T\,(\mathbf{X} - \mathbf{X}_0) \tag{21}$$

$\mathbf{H}(\mathbf{X}, \mathbf{X}_0)$ achieves its global minimum at $\mathbf{X}_0$, called *"recentering point"*, and, in correspondence with it, takes the zero value Fig. 3b. The recentring point can be arbitrarily chosen among the values within the constrained interval. The more the point moves towards the constraint boundaries, the more the recentered barrier function becomes sharp. If the recentering point gets closer to the right side of the constrained set, the magnitude of the slope on the right side becomes larger than on the left side Fig. 3c; the converse holds when the recentering point gets closer to the left boundary.

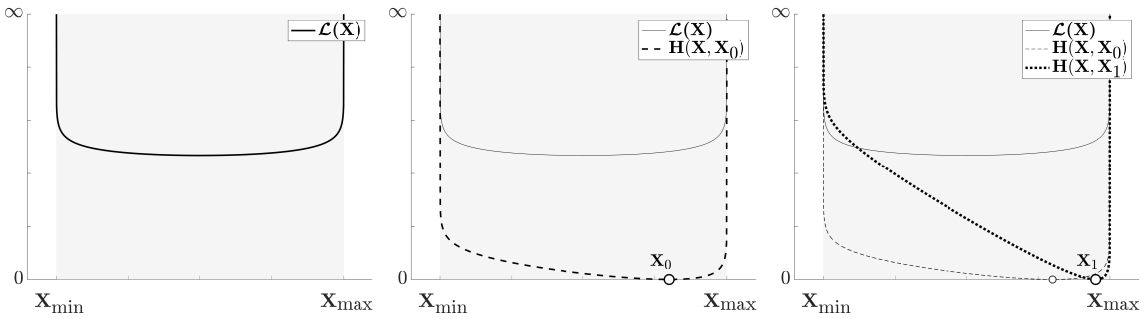

(a) Logarithmic Barrier. (b) Recentered Barrier in $\mathbf{X}_0$. (c) Recentered Barrier in $\mathbf{X}_1$.

Figure 3: One-dimensional Logarithmic Barrier function $\boldsymbol{\mathcal{L}}(\mathbf{X})$, Logarithmic Barrier function $\mathbf{H}(\mathbf{X}, \mathbf{X}_0)$ recentered in $\mathbf{X}_0$ and Logarithmic Barrier function $\mathbf{H}(\mathbf{X}, \mathbf{X}_1)$ recentered in $\mathbf{X}_1$. : constrained region.

IV. METHODOLOGY

This section is devoted to the incorporation of logarithmic barrier functions into Linear Quadratic Differential Games and to the subsequent derivation of the strategies of the players.

Predictive Correction on Recentered Barrier Functions

The recentered barrier function Eq. (21) is discretized over time by explicitly expressing the dependency on the predicted state at time step $(k+1)$ and on the current state at time step (k):

$$\mathbf{W}_{j,(k+1)} = \mathbf{H}_{j,(k+1)} \left(\mathbf{X}_{j,(k+1)}, \mathbf{X}_{j,(k)} \right) \tag{22}$$

for $k = 0, \ldots, N-1$
where $\mathbf{W}_{j,(k+1)}$ is the vector value of the barrier computed at the predicted state $\mathbf{X}_{j,(k+1)}$ and recentered in the current state $\mathbf{X}_{j,(k)}$, associated with s/c$_j$.

A correction in the controls also induces a variation in the vector value of the barrier, according to the notation introduced previously: $\mathbf{W}_{j,(k+1)} = \mathbf{w}_{j,(k+1)} + d\mathbf{w}_{j,(k+1)}$. To express the variation of the vector value of the barrier, a first-order Taylor expansion is performed:

$$\begin{aligned}
\mathbf{W}_{j,(k+1)} &= \mathbf{H}_{j,(k+1)}(\mathbf{x}_{j,(k+1)} + d\mathbf{x}_{j,(k+1)}, \mathbf{x}_{j,(k)} + d\mathbf{x}_{j,(k)}) && (23)\\
&\simeq \mathbf{H}_{j,(k+1)}(\mathbf{x}_{j,(k+1)}, \mathbf{x}_{j,(k)}) + \left[\frac{\partial \mathbf{H}_{j,(k+1)}}{\partial \mathbf{X}_{j,(k+1)}}\right] d\mathbf{x}_{j,(k+1)} + \left[\frac{\partial \mathbf{H}_{j,(k+1)}}{\partial \mathbf{X}_{j,(k)}}\right] d\mathbf{x}_{j,(k)} && (24)\\
&\simeq \mathbf{w}_{j,(k+1)} + \left[\frac{\partial \mathbf{H}_{j,(k+1)}}{\partial \mathbf{X}_{j,(k+1)}}\right] d\mathbf{x}_{j,(k+1)} + \left[\frac{\partial \mathbf{H}_{j,(k+1)}}{\partial \mathbf{X}_{j,(k)}}\right] d\mathbf{x}_{j,(k)} && (25)
\end{aligned}$$

therefore:

$$d\mathbf{w}_{j,(k+1)} = \left[\frac{\partial \mathbf{H}_{j,(k+1)}}{\partial \mathbf{X}_{j,(k+1)}}\right] d\mathbf{x}_{j,(k+1)} + \left[\frac{\partial \mathbf{H}_{j,(k+1)}}{\partial \mathbf{X}_{j,(k)}}\right] d\mathbf{x}_{j,(k)} \tag{26}$$

for $k = 0, \ldots, N-1$.

By enforcing constraints on a second spatial dimension, the recentered barrier becomes a two-dimensional function. When s/c$_j$ moves towards the constraint defined by $\lambda_{\max}$ Fig. 4a, the value of the barrier expressed by $\mathbf{H}_{j,(k+1)}(\mathbf{X}_{j,(k+1)}, \mathbf{X}_{j,(k)})$ increases progressively until a point in which it is more convenient for s/c$_j$ to move in the opposite direction. The barrier is recentered in the state predicted at the previous step, and the resulting function $\mathbf{H}_{j,(k+2)}(\mathbf{X}_{j,(k+2)}, \mathbf{X}_{j,(k+1)})$ imposes a

preferential direction of motion toward the corner formed by the intersection of the constraints $\lambda_{\min}$ and $r_{\min}$ Fig. 4b. s/c $_j$ executes a new portion of trajectory, and the sequence repeats Fig. 4c.

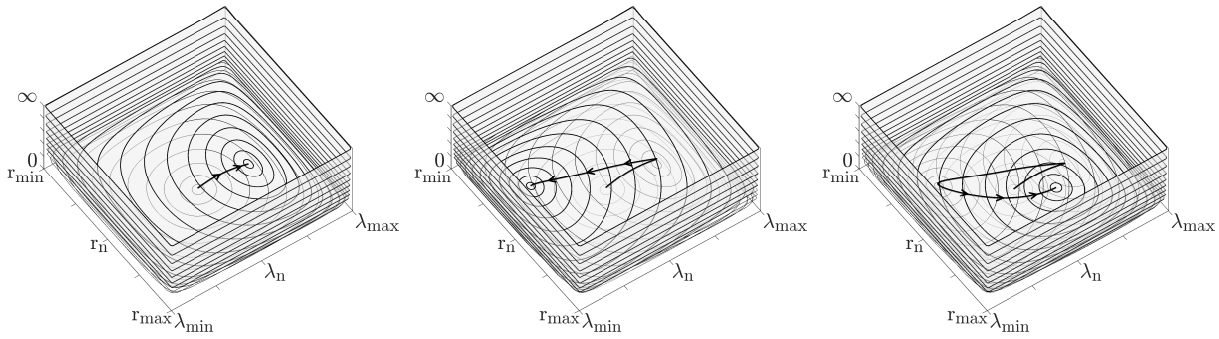

(a) for $k = (\overline{k})$. (b) for $k = (\overline{k}+1)$. (c) for $k = (\overline{k}+2)$.

Figure 4: Dynamics of a two-dimensional Logarithmic Barrier $\mathbf{H}_{j,(k+1)}(\mathbf{X}_{j,(k+1)}, \mathbf{X}_{j,(k)})$ computed in the predicted state $\mathbf{X}_{j,(k+1)}$ and recentered in the current state $\mathbf{X}_{j,(k)}$. ◎: level curves; ⟶ s/c trajectory.

Subsequently, the virtual variation of the vector value of the barrier $\mathbf{W}_{j,(k+1)}$, with respect to the free coordinates $d\mathbf{x}_{j,(k+1)}$ and $d\mathbf{x}_{j,(k)}$, is computed as follows:

$$\delta(d\mathbf{w}_{j,(k+1)}) = \frac{\partial}{\partial d\mathbf{x}_{j,(k+1)}}\Big(\, d\mathbf{w}_{j,(k+1)} \,\Big)\, \delta d\mathbf{x}_{j,(k+1)} \;+\; \frac{\partial}{\partial d\mathbf{x}_{j,(k)}}\Big(\, d\mathbf{w}_{j,(k+1)} \,\Big)\, \delta d\mathbf{x}_{j,(k)} \tag{27}$$

$$= \left(\left[\frac{\partial \mathbf{H}_{j,(k+1)}}{\partial \mathbf{X}_{j,(k+1)}}\right] \left[\frac{\partial d\mathbf{x}_{j,(k+1)}}{\partial d\mathbf{x}_{j,(k+1)}}\right] \;+\; \left[\frac{\partial \mathbf{H}_{j,(k+1)}}{\partial \mathbf{X}_{j,(k)}}\right] \left[\frac{\partial d\mathbf{x}_{j,(k)}}{\partial d\mathbf{x}_{j,(k+1)}}\right] \right) \delta d\mathbf{x}_{j,(k+1)} \;+ \ldots$$

$$+ \left(\left[\frac{\partial \mathbf{H}_{j,(k+1)}}{\partial \mathbf{X}_{j,(k+1)}}\right] \left[\frac{\partial d\mathbf{x}_{j,(k+1)}}{\partial d\mathbf{x}_{j,(k)}}\right] \;+\; \left[\frac{\partial \mathbf{H}_{j,(k+1)}}{\partial \mathbf{X}_{j,(k)}}\right] \left[\frac{\partial d\mathbf{x}_{j,(k)}}{\partial d\mathbf{x}_{j,(k)}}\right] \right) \delta d\mathbf{x}_{j,(k)} \tag{28}$$

$$= \left[\frac{\partial \mathbf{H}_{j,(k+1)}}{\partial \mathbf{X}_{j,(k+1)}}\right] \delta d\mathbf{x}_{j,(k+1)} \;+\; \left[\frac{\partial \mathbf{H}_{j,(k+1)}}{\partial \mathbf{X}_{j,(k)}}\right] \delta d\mathbf{x}_{j,(k)} \tag{29}$$

where $\left[\frac{\partial d\mathbf{x}_{j,(k)}}{\partial d\mathbf{x}_{j,(k+1)}}\right] = \mathbf{0}$ as the variation of the state in the current time step (k) is not influenced by the variation of the state at the next time step $(k+1)$; and $\left[\frac{\partial d\mathbf{x}_{j,(k+1)}}{\partial d\mathbf{x}_{j,(k)}}\right] = \mathbf{0}$ as the free coordinates $d\mathbf{x}_{j,(k+1)}$ and $d\mathbf{x}_{j,(k)}$ are assumed to be independent of each other, therefore the state dynamics Eq. (10) is not directly enforced in the expression of the virtual variation of the recentered barrier. However, as shown in the following subsection, the satisfaction of the state dynamics is imposed through an independent term inside the objective function of the players. Therefore, even if the virtual variation of the recentered barrier does not explicitly contain the state dynamics, it remains consistent with it.

Derivation of the players' strategies

In a Zero-Sum Game, the structure of the objective functions associated with s/c $_1$ Eq. (1) and s/c $_2$ Eq. (2) is antisymmetric: $J_1 = -J_2$. This property allows to describe the game with a single objective function J, which is then expanded in the form of augmented performace index $\tilde{J}$ to enforce the satisfaction of the states dynamics Eq. (11), expressed in the form of equality constraints

through the adjoint variables $\boldsymbol{\lambda}_{1,(k+1)},\ \boldsymbol{\lambda}_{2,(k+1)} \in \mathbb{R}^6$:

$$\begin{aligned}\min_{\substack{\mathbf{U}_{1,(k)},\mathbf{U}_{2,(k)}\\ \in\, \mathbb{U}_1\times\mathbb{U}_2}} \tilde{J} = {} & \frac{1}{2}\mathbf{Y}_{(N)}^T\mathbf{Q}\mathbf{Y}_{(N)} + \frac{1}{2}\sum_{k=0}^{N-1}\mathbf{U}_{1,(k)}^T\mathbf{R}_{1,(k)}\mathbf{U}_{1,(k)} - \frac{1}{2}\sum_{k=0}^{N-1}\mathbf{U}_{2,(k)}^T\mathbf{R}_{2,(k)}\mathbf{U}_{2,(k)} + \dots \\ & + \sum_{k=0}^{N-1}\boldsymbol{\lambda}_{1,(k+1)}^T\left(d\mathbf{x}_{1,(k+1)} - \left[\frac{\partial\mathbf{F}_{1,(k)}}{\partial\mathbf{X}_{1,(k)}}\right]d\mathbf{x}_{1,(k)} - \left[\frac{\partial\mathbf{F}_{1,(k)}}{\partial\mathbf{U}_{1,(k)}}\right]d\mathbf{u}_{1,(k)}\right) + \dots \\ & + \sum_{k=0}^{N-1}\boldsymbol{\lambda}_{2,(k+1)}^T\left(d\mathbf{x}_{2,(k+1)} - \left[\frac{\partial\mathbf{F}_{2,(k)}}{\partial\mathbf{X}_{2,(k)}}\right]d\mathbf{x}_{2,(k)} - \left[\frac{\partial\mathbf{F}_{2,(k)}}{\partial\mathbf{U}_{2,(k)}}\right]d\mathbf{u}_{2,(k)}\right) + \dots \\ & + \sum_{k=0}^{N-1}\boldsymbol{\mu}_{1,(k+1)}^T\mathbf{W}_{1,(k+1)} - \sum_{k=0}^{N-1}\boldsymbol{\mu}_{2,(k+1)}^T\mathbf{W}_{2,(k+1)} \end{aligned} \tag{30}$$

Within the predictive horizon, the optimization problem takes the form of a static game. The actions executed by players determine the behavior of the objective function within the time period $[\,0,\ T\,]$. Since the Nash equilibrium coincides with the saddle point solution of a Zero-Sum Static game [21], by imposing to zero the virtual variation of the augmented performance index $\tilde{J}$ with respect to the free coordinates of the problem $d\mathbf{x}_{1,(k)},\ d\mathbf{x}_{2,(k)},\ d\mathbf{u}_{1,(0)},\ d\mathbf{u}_{2,(0)}$ and by recalling Eqs. (18) and (29), the necessary conditions for the existence of a saddle point solution are derived.

$$\left[\frac{\partial\mathbf{Y}_{(N)}}{\partial\mathbf{X}_{1,(N)}}\right]^T\mathbf{Q}^T(\mathbf{y}_{(N)} + d\mathbf{y}_{(N)}) \ + \ \boldsymbol{\lambda}_{1,(N)} \ + \ \left[\frac{\partial\mathbf{H}_{1,(N)}}{\partial\mathbf{X}_{1,(N)}}\right]^T\boldsymbol{\mu}_{1,(N)} = \mathbf{0} \tag{31}$$

$$\left[\frac{\partial\mathbf{Y}_{(N)}}{\partial\mathbf{X}_{2,(N)}}\right]^T\mathbf{Q}^T(\mathbf{y}_{(N)} + d\mathbf{y}_{(N)}) \ + \ \boldsymbol{\lambda}_{2,(N)} \ + \ \left[\frac{\partial\mathbf{H}_{2,(N)}}{\partial\mathbf{X}_{2,(N)}}\right]^T\boldsymbol{\mu}_{2,(N)} = \mathbf{0} \tag{32}$$

$$\mathbf{R}_{1,(0)}^T(\mathbf{u}_{1,(0)} + d\mathbf{u}_{1,(0)}) \ - \ \left[\frac{\partial\mathbf{F}_{1,(0)}}{\partial\mathbf{U}_{1,(0)}}\right]^T\boldsymbol{\lambda}_{1,(1)} = \mathbf{0} \tag{33}$$

$$\mathbf{R}_{2,(0)}^T(\mathbf{u}_{2,(0)} + d\mathbf{u}_{2,(0)}) \ + \ \left[\frac{\partial\mathbf{F}_{2,(0)}}{\partial\mathbf{U}_{2,(0)}}\right]^T\boldsymbol{\lambda}_{2,(1)} = \mathbf{0} \tag{34}$$

$$\boldsymbol{\lambda}_{1,(k)} \ - \ \left[\frac{\partial\mathbf{F}_{1,(k)}}{\partial\mathbf{X}_{1,(k)}}\right]^T\boldsymbol{\lambda}_{1,(k+1)} = \mathbf{0} \tag{35}$$

$$\boldsymbol{\lambda}_{2,(k)} \ - \ \left[\frac{\partial\mathbf{F}_{2,(k)}}{\partial\mathbf{X}_{2,(k)}}\right]^T\boldsymbol{\lambda}_{2,(k+1)} = \mathbf{0} \tag{36}$$

$$\left[\frac{\partial\mathbf{H}_{1,(k)}}{\partial\mathbf{X}_{1,(k)}}\right]^T\boldsymbol{\mu}_{1,(k)} \ + \ \left[\frac{\partial\mathbf{H}_{1,(k+1)}}{\partial\mathbf{X}_{1,(k)}}\right]^T\boldsymbol{\mu}_{1,(k+1)} = \mathbf{0} \tag{37}$$

$$\left[\frac{\partial\mathbf{H}_{2,(k)}}{\partial\mathbf{X}_{2,(k)}}\right]^T\boldsymbol{\mu}_{2,(k)} \ + \ \left[\frac{\partial\mathbf{H}_{2,(k+1)}}{\partial\mathbf{X}_{2,(k)}}\right]^T\boldsymbol{\mu}_{2,(k+1)} = \mathbf{0} \tag{38}$$

From Eqs. (35) and (36), by recursive substitutions, the dynamics of the adjoint variable $\boldsymbol{\lambda}_{j,(k+1)}$ is obtained as follows:

$$\boldsymbol{\lambda}_{j,(1)} = \left(\left[\frac{\partial\mathbf{F}_{j,(N-1)}}{\partial\mathbf{X}_{j,(N-1)}}\right]\cdot\ \dots\ \cdot\left[\frac{\partial\mathbf{F}_{j,(1)}}{\partial\mathbf{X}_{j,(1)}}\right]\right)^T\boldsymbol{\lambda}_{j,(N)} \tag{39}$$

and similarly, from Eqs. (37) and (38) the dynamics of the adjoint variable $\boldsymbol{\mu}_{j,(k+1)}$ is retrieved:

$$\boldsymbol{\mu}_{j,(N)} = \left(- \left[\frac{\partial \mathbf{H}_{j,(N)}}{\partial \mathbf{X}_{j,(N-1)}}\right]^{-1} \left[\frac{\partial \mathbf{H}_{j,(N-1)}}{\partial \mathbf{X}_{j,(N-1)}}\right] \right)^T \cdot \ \ldots \ \cdot \left(- \left[\frac{\partial \mathbf{H}_{j,(1)}}{\partial \mathbf{X}_{j,(0)}}\right]^{-1} \left[\frac{\partial \mathbf{H}_{j,(0)}}{\partial \mathbf{X}_{j,(0)}}\right] \right)^T \boldsymbol{\mu}_{j,(0)} \quad (40)$$

The expressions of the control correction are isolated from Eqs. (33) and (34):

$$d\mathbf{u}_{1,(0)} = -\ \mathbf{u}_{1,(0)} + \mathbf{E}_{1,(0)} \boldsymbol{\lambda}_{1,(N)} \quad (41)$$

$$d\mathbf{u}_{2,(0)} = -\ \mathbf{u}_{2,(0)} - \mathbf{E}_{2,(0)} \boldsymbol{\lambda}_{2,(N)} \quad (42)$$

where:

$$\mathbf{E}_{1,(0)} = \mathbf{R}_{1,(0)}^{-1} \left[\frac{\partial \mathbf{F}_{1,(0)}}{\partial \mathbf{U}_{1,(0)}}\right]^T \left(\left[\frac{\partial \mathbf{F}_{1,(N-1)}}{\partial \mathbf{X}_{1,(N-1)}}\right] \cdot \ \ldots \ \cdot \left[\frac{\partial \mathbf{F}_{1,(1)}}{\partial \mathbf{X}_{1,(1)}}\right] \right)^T \quad (43)$$

$$\mathbf{E}_{2,(0)} = \mathbf{R}_{2,(0)}^{-1} \left[\frac{\partial \mathbf{F}_{2,(0)}}{\partial \mathbf{U}_{2,(0)}}\right]^T \left(\left[\frac{\partial \mathbf{F}_{2,(N-1)}}{\partial \mathbf{X}_{2,(N-1)}}\right] \cdot \ \ldots \ \cdot \left[\frac{\partial \mathbf{F}_{2,(1)}}{\partial \mathbf{X}_{2,(1)}}\right] \right)^T \quad (44)$$

and then substituted inside Eqs. (31) and (32) where the expression of the variation of the output of the game Eq. (19) is explicitly specified:

$$\left[\frac{\partial \mathbf{Y}_{(N)}}{\partial \mathbf{X}_{1,(N)}}\right]^T \mathbf{Q}^T \big(\mathbf{y}_{(N)} - \mathbf{B}_{(0)} \mathbf{u}_{1,(0)} + \mathbf{B}_{(0)} \mathbf{E}_{1,(0)} \boldsymbol{\lambda}_{1,(N)} - \mathbf{C}_{(0)} \mathbf{u}_{2,(0)} - \mathbf{C}_{(0)} \mathbf{E}_{2,(0)} \boldsymbol{\lambda}_{2,(N)} \big) \ + \ldots$$
$$+ \ \boldsymbol{\lambda}_{1,(N)} \ + \ \left[\frac{\partial \mathbf{H}_{1,(N)}}{\partial \mathbf{X}_{1,(N)}}\right]^T \mathbf{N}_{1,(0)} \ \boldsymbol{\mu}_{1,(0)} = \mathbf{0} \quad (45)$$

$$\left[\frac{\partial \mathbf{Y}_{(N)}}{\partial \mathbf{X}_{2,(N)}}\right]^T \mathbf{Q}^T \big(\mathbf{y}_{(N)} - \mathbf{B}_{(0)} \mathbf{u}_{1,(0)} + \mathbf{B}_{(0)} \mathbf{E}_{1,(0)} \boldsymbol{\lambda}_{1,(N)} - \mathbf{C}_{(0)} \mathbf{u}_{2,(0)} - \mathbf{C}_{(0)} \mathbf{E}_{2,(0)} \boldsymbol{\lambda}_{2,(N)} \big) \ + \ldots$$
$$+ \ \boldsymbol{\lambda}_{2,(N)} \ - \ \left[\frac{\partial \mathbf{H}_{2,(N)}}{\partial \mathbf{X}_{2,(N)}}\right]^T \mathbf{N}_{2,(0)} \ \boldsymbol{\mu}_{2,(0)} = \mathbf{0} \quad (46)$$

where:

$$\mathbf{N}_{1,(0)} = \left(- \left[\frac{\partial \mathbf{H}_{1,(N)}}{\partial \mathbf{X}_{1,(N-1)}}\right]^{-1} \left[\frac{\partial \mathbf{H}_{1,(N-1)}}{\partial \mathbf{X}_{1,(N-1)}}\right] \right)^T \cdot \ \ldots \ \cdot \left(- \left[\frac{\partial \mathbf{H}_{1,(1)}}{\partial \mathbf{X}_{1,(0)}}\right]^{-1} \left[\frac{\partial \mathbf{H}_{1,(0)}}{\partial \mathbf{X}_{1,(0)}}\right] \right)^T \quad (47)$$

$$\mathbf{N}_{2,(0)} = \left(- \left[\frac{\partial \mathbf{H}_{2,(N)}}{\partial \mathbf{X}_{2,(N-1)}}\right]^{-1} \left[\frac{\partial \mathbf{H}_{2,(N-1)}}{\partial \mathbf{X}_{2,(N-1)}}\right] \right)^T \cdot \ \ldots \ \cdot \left(- \left[\frac{\partial \mathbf{H}_{2,(1)}}{\partial \mathbf{X}_{2,(0)}}\right]^{-1} \left[\frac{\partial \mathbf{H}_{2,(0)}}{\partial \mathbf{X}_{2,(0)}}\right] \right)^T \quad (48)$$

The expression of the adjoint variables associated with the enforcement of the state dynamics $\boldsymbol{\lambda}_{1,(N)},\ \boldsymbol{\lambda}_{2,(N)}$ are isolated from Eqs. (45) and (46):

$$\underbrace{\left(\mathbf{I}_{[6\times 6]} + \left[\frac{\partial \mathbf{Y}_{(N)}}{\partial \mathbf{X}_{1,(N)}}\right]^T \mathbf{Q}^T \mathbf{B}_{(0)} \mathbf{E}_{1,(0)} \right)}_{\mathbf{M}_{11}} \boldsymbol{\lambda}_{1,(N)} \ \underbrace{- \left[\frac{\partial \mathbf{Y}_{(N)}}{\partial \mathbf{X}_{1,(N)}}\right]^T \mathbf{Q}^T \mathbf{C}_{(0)} \mathbf{E}_{2,(0)}}_{\mathbf{M}_{12}} \boldsymbol{\lambda}_{2,(N)} \ + \ \ldots$$
$$\underbrace{\left[\frac{\partial \mathbf{Y}_{(N)}}{\partial \mathbf{X}_{1,(N)}}\right]^T \mathbf{Q}^T \big(\mathbf{y}_{(N)} - \mathbf{B}_{(0)} \ \mathbf{u}_{1,(0)} - \mathbf{C}_{(0)} \ \mathbf{u}_{2,(0)} \big) \ + \ \left[\frac{\partial \mathbf{H}_{1,(N)}}{\partial \mathbf{X}_{1,(N)}}\right]^T \mathbf{N}_{1,(0)} \ \boldsymbol{\mu}_{1,(0)}}_{\mathbf{b}_1} = \mathbf{0} \quad (49)$$

$$\underbrace{\left(\mathbf{I}_{[6\times6]} - \left[\frac{\partial \mathbf{Y}_{(N)}}{\partial \mathbf{X}_{2,(N)}}\right]^T \mathbf{Q}^T \mathbf{C}_{(0)} \mathbf{E}_{2,(0)}\right)}_{\mathbf{M}_{22}} \boldsymbol{\lambda}_{2,(N)} \underbrace{+ \left[\frac{\partial \mathbf{Y}_{(N)}}{\partial \mathbf{X}_{2,(N)}}\right]^T \mathbf{Q}^T \mathbf{B}_{(0)} \mathbf{E}_{1,(0)}}_{\mathbf{M}_{21}} \boldsymbol{\lambda}_{1,(N)} + \dots$$

$$\underbrace{\left[\frac{\partial \mathbf{Y}_{(N)}}{\partial \mathbf{X}_{2,(N)}}\right]^T \mathbf{Q}^T \left(\mathbf{y}_{(N)} - \mathbf{B}_{(0)}\, \mathbf{u}_{1,(0)} - \mathbf{C}_{(0)}\, \mathbf{u}_{2,(0)} \right) - \left[\frac{\partial \mathbf{H}_{2,(N)}}{\partial \mathbf{X}_{2,(N)}}\right]^T \mathbf{N}_{2,(0)}\, \boldsymbol{\mu}_{2,(0)}}_{\mathbf{b}_2} = \mathbf{0} \quad (50)$$

The previous equations are then rewritten as a linear system in the unknowns $[\ \boldsymbol{\lambda}_{1,(N)},\ \boldsymbol{\lambda}_{2,(N)}\ ]^T$ whose expressions are extracted as follows:

$$\begin{pmatrix} \boldsymbol{\lambda}_{1,(N)} \\ \boldsymbol{\lambda}_{2,(N)} \end{pmatrix} = - \begin{bmatrix} \mathbf{M}_{11} & \mathbf{M}_{12} \\ \mathbf{M}_{21} & \mathbf{M}_{22} \end{bmatrix}^{-1} \begin{pmatrix} \boldsymbol{b}_1 \\ \boldsymbol{b}_2 \end{pmatrix} \quad (51)$$

where $\mathbf{M}_{11},\ \mathbf{M}_{12},\ \mathbf{M}_{21},\ \mathbf{M}_{22} \in \mathbb{R}^{6\times6}$, and $\mathbf{b}_1,\ \mathbf{b}_2 \in \mathbb{R}^6$.

By inserting $\boldsymbol{\lambda}_{1,(N)},\ \boldsymbol{\lambda}_{2,(N)}$ into Eqs. (41) and (42) the expressions of the control corrections that ensure the establishment of a constrained Nash equilibrium within the predictive horizon are retrieved. As a consequence, the solution of the overall game is made by the composition of optimal solutions according to the receding time-horizon technique.

V. STRUCTURE OF THE ALGORITHM

In a Nash equilibrium both players are modeled as separate entities that do not exchange information about their strategies, but they can access to the system state, composed of the individual states of each spacecraft, prior to executing their respective moves. The moves are performed simultaneously, and instantaneously they change the state of the system. The updated state of the system is then observed by the players that recompute new control corrections and apply them following an iterative scheme until the end of the game. In Fig. 5, the iterative steps for a generic player j are shown, regardless of whether his task is to pursue or evade.

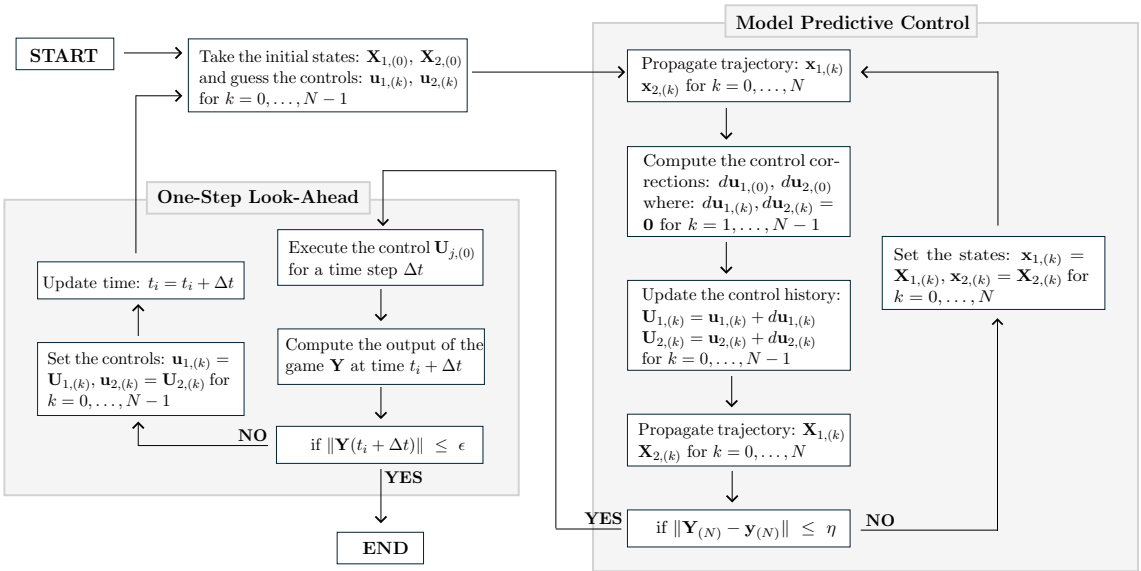

Figure 5: Iterative subscheme for a generic player j.

The core of the algorithm consists of two sequential steps, the Model Predictive Control (MPC) and the One-Step Look-Ahead Fig. 6. The MPC is an iterative scheme that allows to compute the control corrections that ensure the establishment of an equilibrium within the predictive horizon. In the One-Step Look-Ahead, instead, each player applies his respective control correction, checks whether the stopping condition is met, updates his trajectory and strategy, and then shifts forward the time of the game. If the difference between the value of the corrected output of the game $\mathbf{Y}_{(N)}$, computed at the end of the predictive horizon, and the uncorrected one $\mathbf{y}_{(N)}$ is greater than a certain threshold η, the predictive step continues. The trajectories propagated using control corrections that do not satisfy the condition imposed by the MPC become the old ones $\mathbf{x}_{1,(k)}, \mathbf{x}_{2,(k)}$, which are then used to compute the new control correction Eqs. (41) and (42). If the condition imposed by the MPC is satisfied, the predictive control loop stops, and the algorithm advances to the One-Step Look-Ahead block.

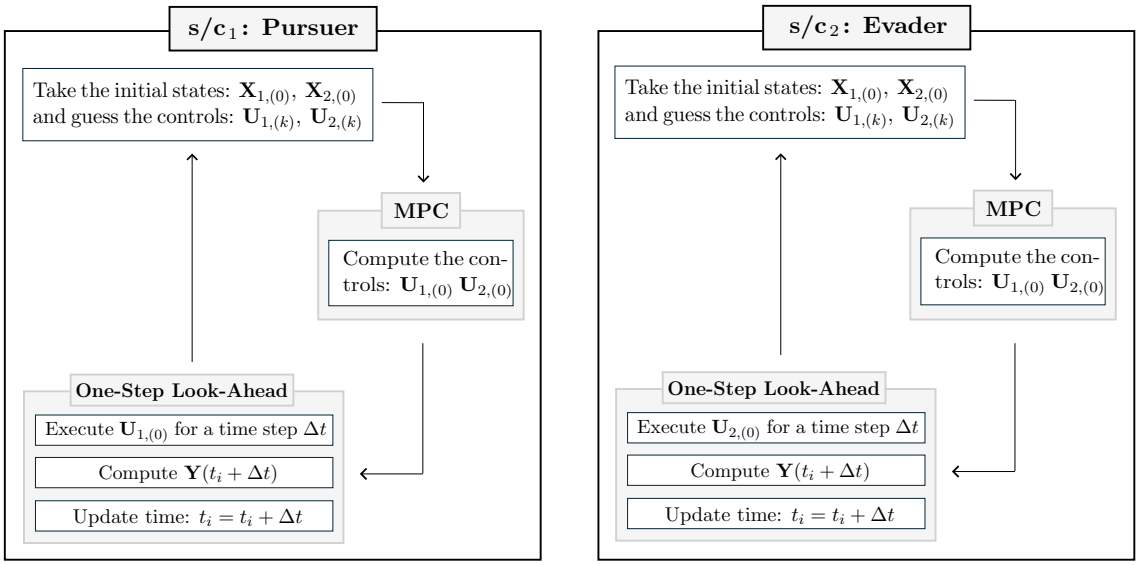

Figure 6: Structure of the algorithm for a Nash equilibrium formulation.

A fourth-order Runge-Kutta integration scheme is used to propagate the trajectories of the players. Proper adimensionalization techniques and damped Newton methods are used to reduce the computational time and to improve the likelihood of convergence of the MPC iterative loop. The end of the game occurs when the distance between the spacecraft is approximately 4 m. The stopping condition marking the event is triggered by the dimensionless quantity ϵ.

VI. SIMULATION RESULTS

This section presents the numerical results obtained using the proposed methodology. Both spacecraft are initially placed on a circular geostationary orbit with zero inclination and are separated by an initial phase angle. The initial position vectors are reported in the boxes summarizing the simulation parameters adopted for each example. The weighting matrices are selected to yield meaningful results and to favour complex interactions between the players throughout the game evolution. An unconstrained pursuit–evasion game is first analyzed as a reference case, followed by constrained scenarios designed to assess the impact of orbital-slot limitations and model parameters on the outcome of the game.

The unconstrained game terminates with a capture after approximately two days, as illustrated in Fig. 7, with the corresponding control histories shown in Fig. 7.1. The resulting trajectories span more than 200 km with respect to the nominal geostationary radius, highlighting the large spatial envelope associated with unconstrained evasive maneuvers.

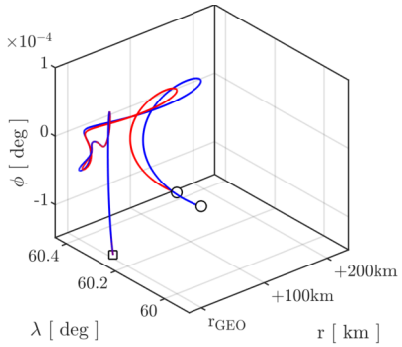

(a) trajectories on 3D view.

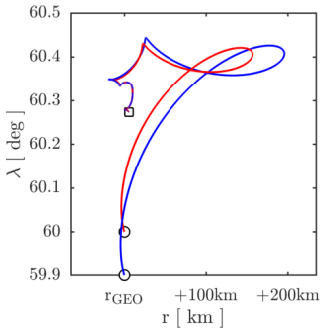

(b) trajectories on $r - \lambda$ view.

$\mathbf{Q} = 1e-4\times\ \mathbf{I}$;
$\mathbf{R}_{1,(0)} = 1e8\times\ \mathbf{I}$; $\mathbf{R}_{2,(0)} = 1.25e8\times\ \mathbf{I}$;

Predictive horizon: T = 1 h; N = 100;
Stop conditions: $\epsilon = 1e-07$; $\eta = 1e-08$;

Initial states
s/c$_1$: [42165.8 km, 59.90 deg, 0.00 deg,
0.00 km/s, 0.00 deg/s, 0.00 deg/s];
s/c$_2$: [42165.8 km, 60.00 deg, 0.00 deg,
0.00 km/s, 0.00 deg/s, 0.00 deg/s];

Capture realized: $\|\mathbf{Y}(t_f)\| = 4.19$ m
Duration of the game:
2 days, 4 h, 4 min, 12 sec

(c) simulation parameters.

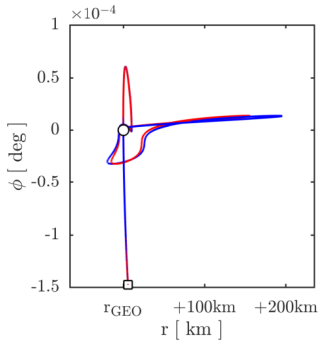

(d) trajectories on $r - \phi$ view.

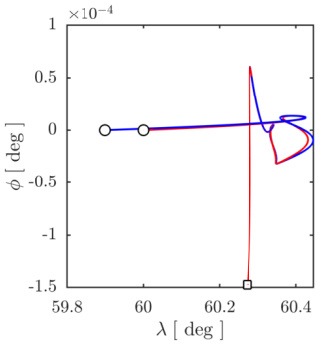

(e) trajectories on $\lambda - \phi$ view.

Figure 7: Nash equilibrium solution of the unconstrained pursuit-evasion game.
— s/c$_1$: pursuer; — s/c$_2$: evader; ○: initial point; □: final point.

The most significant variations in the control inputs occur during the initial phase of the engagement. As the engagement progresses, all control components gradually converge toward zero, reflecting the players' tendency to minimize control effort while establishing equilibrium solutions within the game.

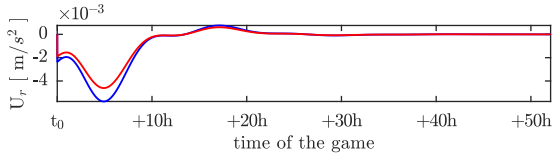

(f) control strategies on r coordinate.

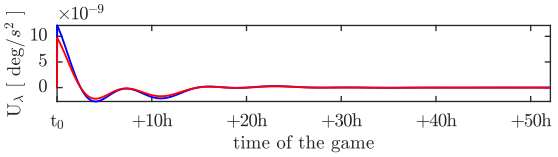

(g) control strategies on λ coordinate.

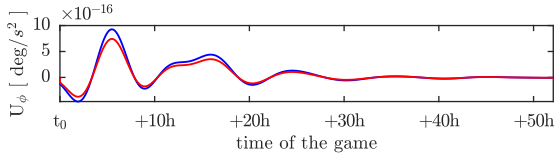

(h) control strategies on ϕ coordinate.

Figure 7.1: Control strategies of the unconstrained pursuit-evasion game.
— $\mathbf{U}_{s/c\,1}$: pursuer; — $\mathbf{U}_{s/c\,2}$: evader.

An admissible region centered at the evader's initial position is then introduced, with maximum deviations of 20 km in range and 0.05 deg in both latitude and longitude. The corresponding solution of the constrained game, shown in Fig. 8, demonstrates that the enforcement of path constraints on the motion of the evader does not inherently simplify the capture process for the pursuer. Except for the initial transient, the pursuer refrains from a direct attack and instead remains in orbit around the evader, without achieving capture. This configuration represents a dynamic equilibrium in which the pursuer is prepared to initiate a more aggressive maneuver if the evader unilaterally modifies its current strategy.

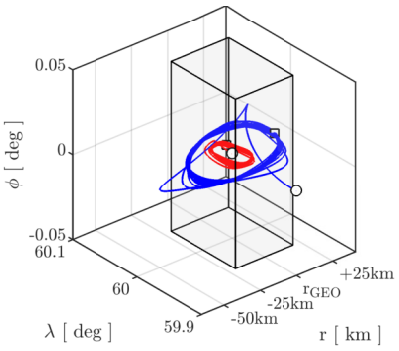

(a) trajectories on 3D view.

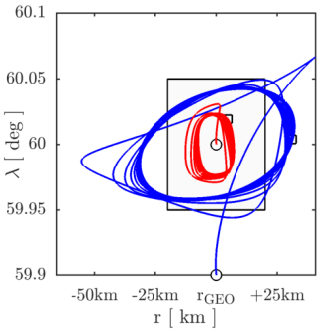

(b) trajectories on $r - \lambda$ view.

$\mathbf{Q} = 1e-4\times\ \mathbf{I}$;
$\mathbf{R}_{1,(0)} = 1e8\times\ \mathbf{I}$; $\mathbf{R}_{2,(0)} = 1.25e8\times\ \mathbf{I}$;

Predictive horizon: T = 0.5 h; N = 50;
Stop conditions: $\epsilon = 1e-07$; $\eta = 1e-08$;

Initial states
s/c$_1$: [42165.8 km, 59.90 deg, 0.00 deg,
0.00 km/s, 0.00 deg/s, 0.00 deg/s];
s/c$_2$: [42165.8 km, 60.00 deg, 0.00 deg,
0.00 km/s, 0.00 deg/s, 0.00 deg/s];
$\boldsymbol{\mu}_{2,(0)} = 1\times$ [1, 1, 1, 0, 0, 0];

Capture not realized: $\|\mathbf{Y}(t_f)\| = 28566.3$ m
Duration of the game:
8 days, 7 h, 59 min, 60 sec

(c) simulation parameters.

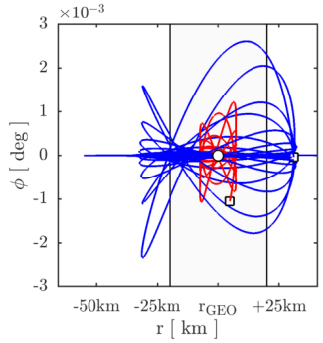

(d) trajectories on $r - \phi$ view.

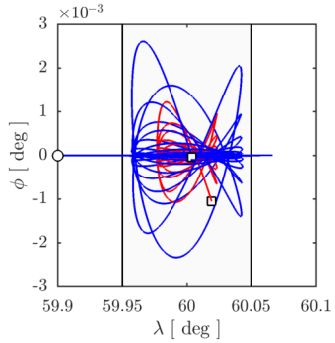

(e) trajectories on $\lambda - \phi$ view.

Figure 8: Nash equilibrium solution of the constrained pursuit-evasion game. — s/c$_1$: pursuer; — s/c$_2$: evader; ○: initial point; □: final point; ▭: orbital slot s/c$_2$.

The associated control profiles, reported in Fig. 8.1, exhibit oscillatory behavior around zero, with the latitudinal component showing a progressive increase in amplitude.

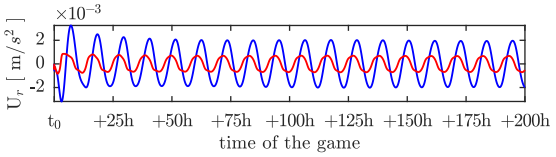

(f) control strategies on r coordinate.

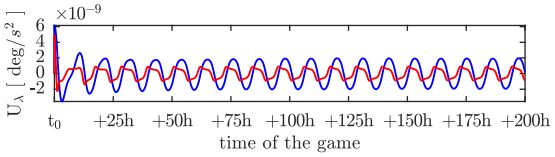

(g) control strategies on λ coordinate.

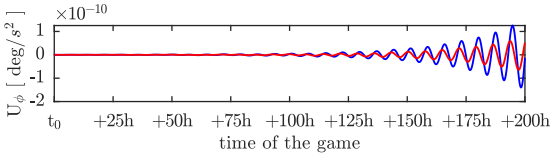

(h) control strategies on ϕ coordinate.

Figure 8.1: Control strategies of the constrained pursuit-evasion game. — $\mathbf{U}_{s/c\,1}$: pursuer; — $\mathbf{U}_{s/c\,2}$: evader.

The evolution of the game is strongly influenced by the parameters governing the barrier function. Increasing the initial value of the adjoint variable $\boldsymbol{\mu}_{2,(0)}$ confines the engagement closer to the center of the evader's orbital slot, as shown in Fig. 9. Under this configuration, the evader successfully performs evasive maneuvers that significantly delay capture.

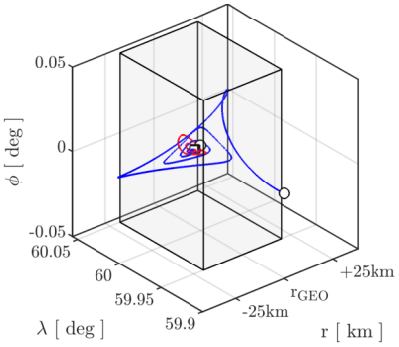

(a) trajectories on 3D view.

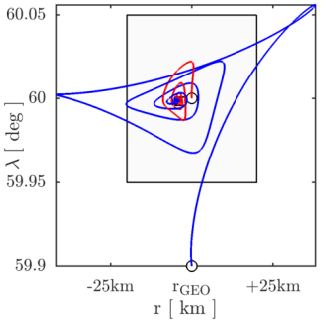

(b) trajectories on $r - \lambda$ view.

$\mathbf{Q} = 1e-4\times\ \mathbf{I}$;
$\mathbf{R}_{1,(0)} = 1e8\times\ \mathbf{I}$; $\mathbf{R}_{2,(0)} = 1.25e8\times\ \mathbf{I}$;

Predictive horizon: T = 0.5 h; N = 50;
Stop conditions: $\epsilon = 1e-07$; $\eta = 1e-08$;

Initial states
s/c$_1$: [42165.8 km, 59.90 deg, 0.00 deg, 0.00 km/s, 0.00 deg/s, 0.00 deg/s];
s/c$_2$: [42165.8 km, 60.00 deg, 0.00 deg, 0.00 km/s, 0.00 deg/s, 0.00 deg/s];
$\boldsymbol{\mu}_{2,(0)} = 2\times$ [1, 1, 1, 0, 0, 0];

Capture not realized: $\|\mathbf{Y}(t_f)\| = 792.74$ m
Duration of the game:
8 days, 7 h, 59 min, 60 sec

(c) simulation parameters.

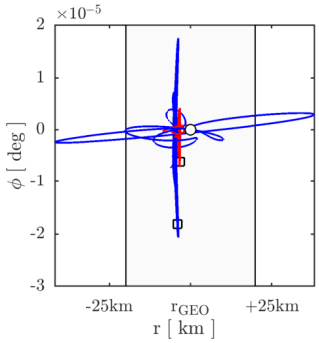

(d) trajectories on $r - \phi$ view.

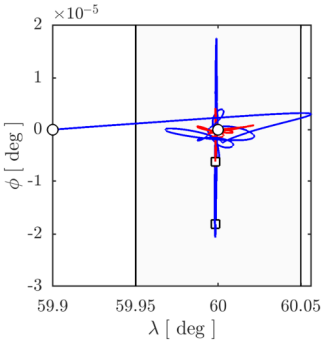

(e) trajectories on $\lambda - \phi$ view.

Figure 9: Nash equilibrium solution of the constrained pursuit-evasion game. — s/c$_1$: pursuer; — s/c$_2$: evader; ○: initial point; □: final point; ▭: orbital slot s/c$_2$.

Conversely, reducing $\boldsymbol{\mu}_{2,(0)}$ allows the evader to approach the boundaries of its admissible region, leading to the establishment of an equilibrium in which the pursuer moves around the evader, remaining outside the orbital slot of the opponent Fig. 10. If the evader unilaterally modify the equilibrium, the pursuer is ready to change its strategy into a more aggressive one, analogously to the example illustrated in Fig. 8.

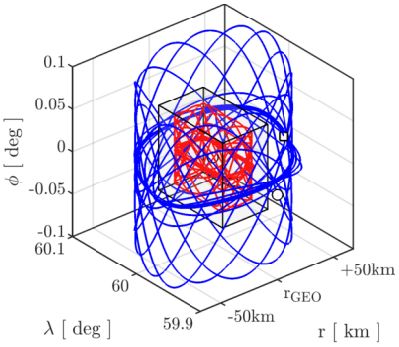

(a) trajectories on 3D view.

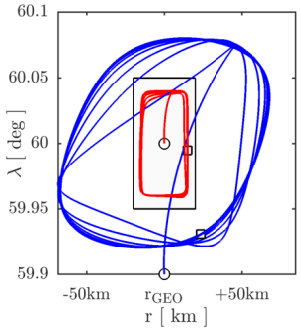

(b) trajectories on $r - \lambda$ view.

$\mathbf{Q} = 1e-4\times\ \mathbf{I}$;
$\mathbf{R}_{1,(0)} = 1e8\times\ \mathbf{I}$; $\mathbf{R}_{2,(0)} = 1.25e8\times\ \mathbf{I}$;

Predictive horizon: T = 0.5 h; N = 50;
Stop conditions: $\epsilon = 1e-07$; $\eta = 1e-08$;

Initial states
s/c$_1$: [42165.8 km, 59.90 deg, 0.00 deg, 0.00 km/s, 0.00 deg/s, 0.00 deg/s];
s/c$_2$: [42165.8 km, 60.00 deg, 0.00 deg, 0.00 km/s, 0.00 deg/s, 0.00 deg/s];
$\boldsymbol{\mu}_{2,(0)} = 0.4\times$ [1, 1, 1, 0, 0, 0];

Capture not realized: $\|\mathbf{Y}(t_f)\| = 74526.3$ m
Duration of the game:
8 days, 7 h, 59 min, 60 sec

(c) simulation parameters.

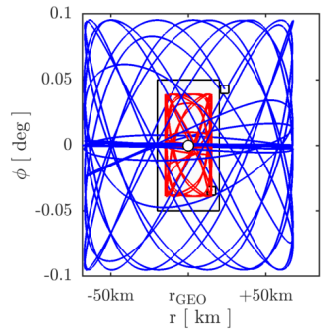

(d) trajectories on $r - \phi$ view.

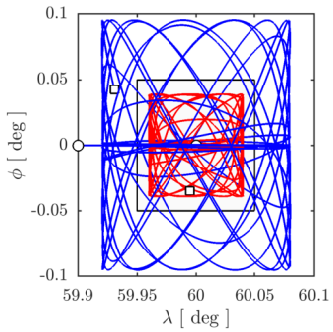

(e) trajectories on $\lambda - \phi$ view.

Figure 10: Nash equilibrium solution of the constrained pursuit-evasion game. — s/c$_1$: pursuer; — s/c$_2$: evader; ○: initial point; □: final point; ▭: orbital slot s/c$_2$.

To force the dynamics of the game toward capture, the weighting matrices $\mathbf{Q}$, $\mathbf{R}_{1,(0)}$, $\mathbf{R}_{2,(0)}$ are modified, as illustrated in Fig. 11. In this case, the pursuer enters the evader's orbital slot, initiating a spiraling motion involving both spacecraft that ultimately results in capture after approximately two days.

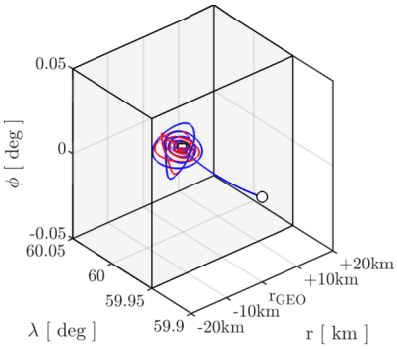

(a) trajectories on 3D view.

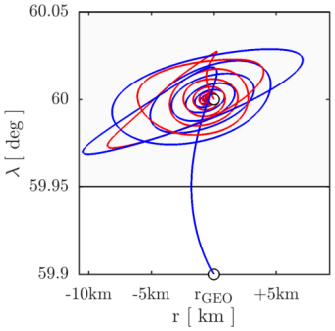

(b) trajectories on $r - \lambda$ view.

$\mathbf{Q} = 1e-3\times\ \mathbf{I}$;
$\mathbf{R}_{1,(0)} = 1e8\times\ \mathbf{I}$; $\mathbf{R}_{2,(0)} = 1.25e8\times\ \mathbf{I}$;

Predictive horizon: T = 0.5 h; N = 50;
Stop conditions: $\epsilon = 1e-07$; $\eta = 1e-08$;

Initial states
s/c$_1$: [42165.8 km, 59.90 deg, 0.00 deg, 0.00 km/s, 0.00 deg/s, 0.00 deg/s];
s/c$_2$: [42165.8 km, 60.00 deg, 0.00 deg, 0.00 km/s, 0.00 deg/s, 0.00 deg/s];
$\boldsymbol{\mu}_{2,(0)} = 0.6 \times$ [1, 1, 1, 0, 0, 0];

Capture realized: $\|\mathbf{Y}(t_f)\| = 4.20$ m
Duration of the game:
2 days, 6 h, 1 min, 48 sec

(c) simulation parameters.

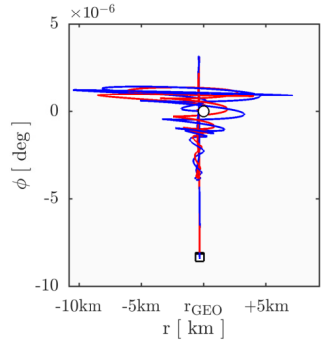

(d) trajectories on $r - \phi$ view.

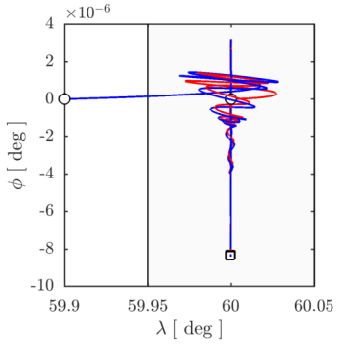

(e) trajectories on $\lambda - \phi$ view.

Figure 11: Nash equilibrium solution of the constrained pursuit-evasion game. — s/c$_1$: pursuer; — s/c$_2$: evader; ○: initial point; □: final point; ▭: orbital slot s/c$_2$.

Nevertheless, the outcome of the game remains highly sensitive to the specific parameter settings, as demonstrated in Fig. 12, where a variation in $\boldsymbol{\mu}_{2,(0)}$ alters the equilibrium and leads to an evasion instead of capture. Compared to the behavior observed in Fig. 11, the evader in this case successfully executes an evasive maneuver that reshapes the overall envelope of the game, transitioning from the $r - \lambda$ plane to the $r - \phi$ plane. The evader subsequently initiates an oscillatory motion toward one of the boundaries of its orbital slot, followed by the pursuer. As the engagement evolves, two

possible scenarios may arise: either the evader continues approaching the slot boundary until it becomes constrained between the pursuer on one side and the admissible-region limit on the other side, ultimately resulting in capture, or it redirects toward another corner of the orbital slot, with the pursuer maintaining the chase until propellant limitations prevent further maneuvering by one of the two satellites.

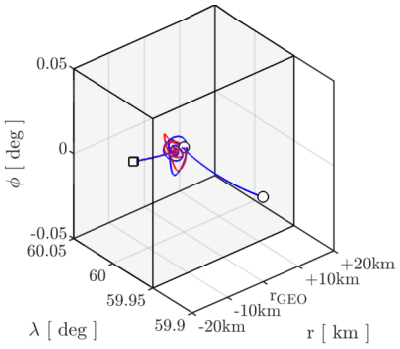

(a) trajectories on 3D view.

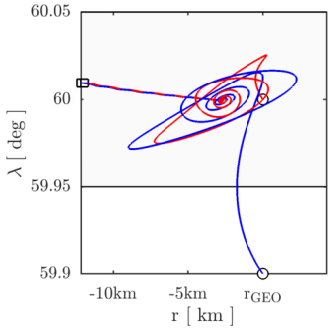

(b) trajectories on $r - \lambda$ view.

$\mathbf{Q} = 1e-3\times\ \mathbf{I}$;
$\mathbf{R}_{1,(0)} = 1e8\times\ \mathbf{I}$; $\mathbf{R}_{2,(0)} = 1.25e8\times\ \mathbf{I}$;

Predictive horizon: T = 0.5 h; N = 50;
Stop conditions: $\epsilon = 1e-07$; $\eta = 1e-08$;

Initial states
s/c$_1$: [42165.8 km, 59.90 deg, 0.00 deg, 0.00 km/s, 0.00 deg/s, 0.00 deg/s];
s/c$_2$: [42165.8 km, 60.00 deg, 0.00 deg, 0.00 km/s, 0.00 deg/s, 0.00 deg/s];
$\boldsymbol{\mu}_{2,(0)} = 1\times$ [1, 1, 1, 0, 0, 0];

Capture not realized: $\|\mathbf{Y}(t_f)\| = 225.66$ m
Duration of the game:
8 days, 7 h, 59 min, 60 sec

(c) simulation parameters.

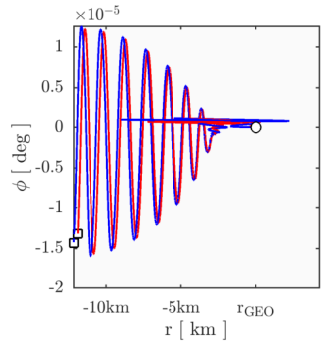

(d) trajectories on $r - \phi$ view.

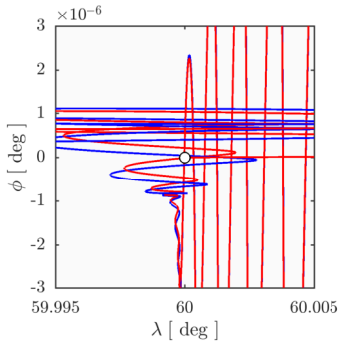

(e) trajectories on $\lambda - \phi$ view.

Figure 12: Nash equilibrium solution of the constrained pursuit-evasion game. — s/c$_1$: pursuer; — s/c$_2$: evader; ○: initial point; □: final point; ▭: orbital slot s/c$_2$.

In addition to model parameters, the initial relative configuration of the players, at the instant in which the pursuer starts its offensive maneuver, plays a critical role in determining the game outcome. When the pursuer is initially shifted forward in longitude with respect to the evader Fig. 13c, capture is achieved in less than 20 hours, effectively preventing the evader from executing meaningful evasive maneuvers. Similar results are observed when the pursuer is positioned ahead of the evader along the radial direction, within the same orbital plane.

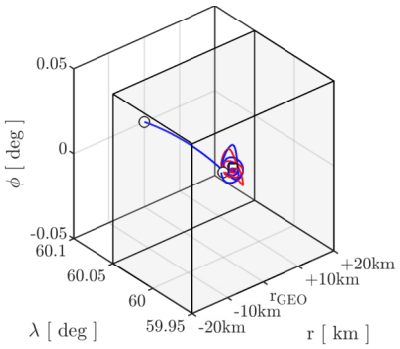

(a) trajectories on 3D view.

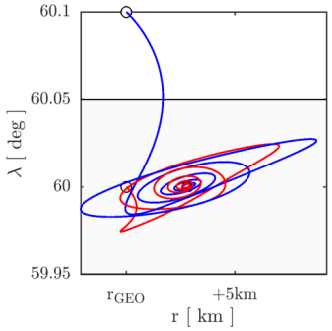

(b) trajectories on $r - \lambda$ view.

$\mathbf{Q} = 1e-3\times\ \mathbf{I}$;
$\mathbf{R}_{1,(0)} = 1e8\times\ \mathbf{I}$; $\mathbf{R}_{2,(0)} = 1.25e8\times\ \mathbf{I}$;

Predictive horizon: T = 0.5 h; N = 50;
Stop conditions: $\epsilon = 1e-07$; $\eta = 1e-08$;

Initial states
s/c$_1$: [42165.8 km, 60.10 deg, 0.00 deg, 0.00 km/s, 0.00 deg/s, 0.00 deg/s];
s/c$_2$: [42165.8 km, 60.00 deg, 0.00 deg, 0.00 km/s, 0.00 deg/s, 0.00 deg/s];
$\boldsymbol{\mu}_{2,(0)} = 1\times$ [1, 1, 1, 0, 0, 0];

Capture realized: $\|\mathbf{Y}(t_f)\| = 2.32$ m
Duration of the game:
0 days, 17 h, 17 min, 60 sec

(c) simulation parameters.

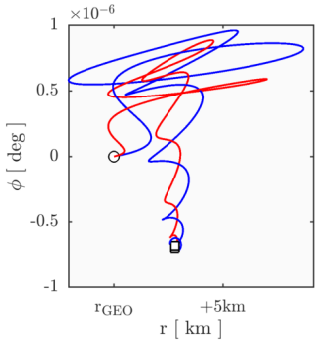

(d) trajectories on $r - \phi$ view.

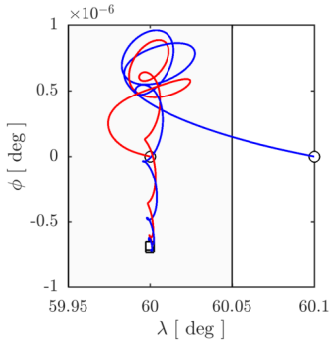

(e) trajectories on $\lambda - \phi$ view.

Figure 13: Nash equilibrium solution of the constrained pursuit-evasion game. — s/c$_1$: pursuer; — s/c$_2$: evader; ○: initial point; □: final point; ▭: orbital slot s/c$_2$.

The robustness and versatility of the proposed method are further demonstrated by considering scenarios in which both spacecraft are simultaneously constrained within distinct admissible regions. To enable the evolution of the game over time, the admissible regions are modeled to partially intersect. As long as the evader remains within space common to both admissible regions, the game continues. When the evader approaches the boundary of its admissible region, the recentered barrier function deflects it back into the shared domain, as shown in Fig. 14b. Once it returns to the common region, the pursuer performs an additional aggressive maneuver, forcing the evader to retreat once again toward the safe zone of its admissible region. The game ultimately terminates when no admissible control action allows the pursuer to further reduce the distance without violating its own constraints.

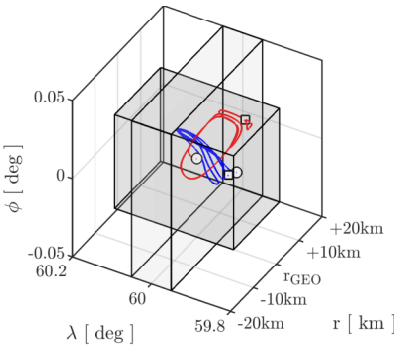

(a) trajectories on 3D view.

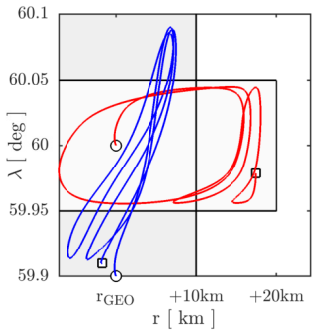

(b) trajectories on $r - \lambda$ view.

$\mathbf{Q} = 1e-4\times\ \mathbf{I}$;
$\mathbf{R}_{1,(0)} = 1e8\times\ \mathbf{I}$; $\mathbf{R}_{2,(0)} = 1.25e8\times\ \mathbf{I}$;

Predictive horizon: T = 0.5 h; N = 50;
Stop conditions: $\epsilon = 1e-07$; $\eta = 1e-08$;

Orbital slot s/c$_1$:
max: [42175.8 km, 60.15 deg, 0.03 deg];
min: [42155.8 km, 59.85 deg, −0.03 deg];
$\boldsymbol{\mu}_{1,(0)} = 0.1 \times [\ 1,\ 1,\ 1,\ 0,\ 0,\ 0\ ]$;

Orbital slot s/c$_2$:
max: [42185.8 km, 60.05 deg, 0.05 deg];
min: [42145.8 km, 59.95 deg, −0.05 deg];
$\boldsymbol{\mu}_{2,(0)} = 0.1 \times [\ 1,\ 1,\ 1,\ 0,\ 0,\ 0\ ]$;

max iterations MPC reached
Capture not realized

(c) simulation parameters.

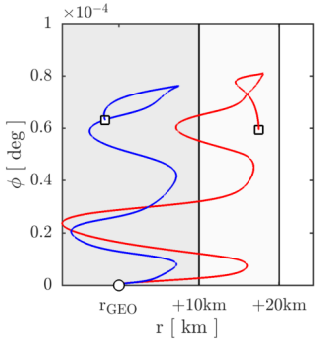

(d) trajectories on $r - \phi$ view.

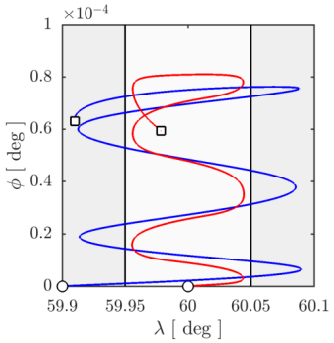

(e) trajectories on $\lambda - \phi$ view.

Figure 14: Nash equilibrium solution of the constrained pursuit-evasion game. — s/c$_1$: pursuer; — s/c$_2$: evader; ○: initial point; □: final point; ▭: orbital slot s/c$_1$; ▭: orbital slot s/c$_2$.

VII. CONCLUSIONS

This paper investigated a constrained orbital pursuit–evasion problem formulated as a linear–quadratic differential game and addressed through an extension of the Model Predictive Static Programming (MPSP) framework. Path constraints were incorporated by means of recentered logarithmic barrier functions, enabling the treatment of operational limitations such as orbital-slot confinement. The proposed approach allows constraints to be imposed on the evader, the pursuer, or both players simultaneously, significantly influencing the evolution of the game and, in most cases, delaying capture. Numerical simulations conducted in the geostationary regime demonstrate that the resulting strategies are highly sensitive to both model parameters and the relative configuration of the players at the beginning of the engagement. Depending on these factors, the game may converge to capture, establish a bounded equilibrium, or result in successful evasion. Due to the generality of the proposed formulation, alternative representations of the equations of motion may be adopted to model the dynamics of the players, while preserving the analytical iterative structure of the solution. The methodology presented in this work therefore provides a consistent and flexible framework for the analysis of constrained orbital pursuit–evasion scenarios. Future work will focus on extending the proposed approach to accommodate constraints on velocity and control variables, investigating the incorporation of state uncertainty for both players, and modeling equilibrium formulations within a nonzero-sum game framework.

REFERENCES

[1] R. Isaacs, *Differential Games*. New York: Wiley, 1965.

[2] J. V. Breakwell and A. W. Merz, "Minimum required capture radius in a coplanar model of the aerial combat problem," *AIAA Journal*, vol. 15, no. 8, pp. 1089–1094, 1977. DOI: 10.2514/3.7399.

[3] K. Horie and B. A. Conway, "Optimal fighter pursuit–evasion maneuvers found via two-sided optimization," *Journal of Guidance, Control, and Dynamics*, vol. 29, no. 1, pp. 105–112, 2006. DOI: 10.2514/1.3960.

[4] M. H. Breitner, H. J. Pesch, and W. Grimm, "Complex differential games of pursuit–evasion type with state constraints, part 1: Necessary conditions for open-loop strategies," *Journal of Optimization Theory and Apllications*, vol. 3, no. 78, pp. 419–441, 1993. DOI: 10.1007/BF00939876.

[5] M. H. Breitner, H. J. Pesch, and W. Grimm, "Complex differential games of pursuit-evasion type with state constraints, part 2: Numerical computation of open-loop strategies," *Journal of Optimization Theory and Applications*, vol. 3, no. 78, pp. 443–463, 1993. DOI: 10.1007/BF00939877.

[6] M. Vasile and F. Bernelli Zazzera, "Direct multiphase optimisation of multiobjective trajectory design problems," in *AAS/AIAA Space Flight Mechanics Meeting*, American Astronautical Society, San Antonio, Texas, Jan. 2002.

[7] B. A. Conway and K. Horie, "A new collocation-based method for solving pursuit–evasion (differential games) problems," *Advances in the Astronautical Sciences*, vol. 109, no. III, 2002.

[8] B. Jarmark, A. W. Merz, and J. V. Breakwell, "The variable-speed tail-chase aerial combat problem," *Journal of Guidance, Control, and Dynamics*, vol. 4, no. 3, pp. 323–328, 1981. DOI: 10.2514/3.19738.

[9] B. Jarmark and C. Hillberg, "Pursuit-evasion between two realistic aircraft," *Journal of Guidance, Control, and Dynamics*, vol. 7, no. 6, pp. 690–694, 1984. DOI: 10.2514/3.19914.

[10] P. Pontani and B. A. Conway, "Numerical solution of the three-dimensional orbital pursuit–evasion game," *Journal of Guidance, Control, and Dynamics*, vol. 32, no. 2, pp. 474–487, 2009. DOI: 10.2514/1.37962.

[11] P. K. A. Menon and A. J. Calise, "Interception, evasion, rendezvous and velocity-to-be-gained guidance for spacecraft," *AIAA Guidance, Navigation and Control Conference*, vol. 1, pp. 334–341, Aug. 1987. DOI: 10.2514/6.1987-2318.

[12] P. K. A. Menon and A. J. Calise, "Guidance laws for spacecraft pursuit - evasion and for rendezvous," *AIAA Guidance, Navigation and Control Conference*, vol. 2, pp. 688–697, Aug. 1988. DOI: 10.2514/6.1988-4134.

[13] A. Jagat and J. A. Sinclair, "Nonlinear control for spacecraft pursuit- evasion game using state-dependent riccati equation method," *IEEE Transactions on Aerospace and Electronic Systems*, vol. 56, no. 6, pp. 3032–3042, 2017. DOI: 10.1109/TAES.2017.2725498.

[14] R. Padhy and M. Kothari, "Model predictive static programming: A computationally efficient technique for suboptimal control design," *International Journal of Innovative Computing, Information and Control*, vol. 5, no. 2, pp. 399–411, 2009.

[15] Y. Liu, C. Li, J. Jiang, and Y. Zhang, "A model predictive Stackelberg solution to orbital pursuit-evasion game," *Chinese Journal of Aeronautics*, vol. 38, no. 2, 2025. DOI: 10.1016/j.cja.2024.08.029.

[16] L. Hengnian, *Geostationary Satellites Collocation*, 1st Edition. Heidelberg: Springer Berlin, 2014.

[17] P. V. Reddy and G. Zaccour, "Feedback nash equilibria in linear-quadratic difference games with constraints," *IEEE Transactions on Automatic Control*, vol. 62, no. 2, pp. 590–604, 2017. DOI: 10.1109/TAC.2016.2555879.

[18] J. Li, S. Sojoudi, C. Tomlin, and D. Fridovich-Keil, *The computation of approximate feedback stackelberg equilibria in multi-player nonlinear constrained dynamic games*, 2025. DOI: 10.48550/arXiv.2401.15745.

[19] L. Zhao, Y. Zhang, and Z. Dang, "PRD-MADDPG: An efficient learning-based algorithm for orbital pursuit-evasion game with impulsive maneuvers," *Advances in Space Research*, vol. 72, no. 2, pp. 211–230, Jul. 2023. DOI: 10.1016/j.asr.2023.03.014.

[20] A. G. Wills and W. P. Heath, "Barrier function based model predictive control," *Automatica*, vol. 40, pp. 1415–1422, 2004. DOI: 10.1016/j.automatica.2004.03.002.

[21] T. Basar and O. G. J., *Dynamic Noncoopeartive Game Theory, 2nd Edition*. Society for Industrial and Applied Mathematics, 1998. DOI: 10.1137/1.9781611971132.

[22] M. Maestrini and S. Carcano, "Polynomial guidance laws for robust fuel optimal station-keeping of geostationary satellites," *Acta Astronautica*, vol. 236, pp. 173–187, Nov. 2025. DOI: 10.1016/j.actaastro.2025.06.047.

[23] J. A. Rossiter, *Model-Based Predictive Control: A Practical Approach*. New York: CRC Press, 2003, pp. 1–57.